Available online at www.sciencedirect.com
ScienceDirect
Journal of Molecular Catalysis A: Chemical 280 (2008) 68–80
JOURNAL OF MOLECULAR CATALYSIS A: CHEMICAL
www.elsevier.com/locate/molcata

DFT calculations, DRIFT spectroscopy and kinetic studies on the hydrolysis of isocyanic acid on the TiO_2-anatase (1 0 1) surface

Izabela Czekaj *, Oliver Kröcher, Gaia Piazzesi

Paul Scherrer Institute, 5232 Villigen PSI, Switzerland

Received 2 August 2007; received in revised form 22 October 2007; accepted 23 October 2007
Available online 30 October 2007

Abstract

The co-adsorption of isocyanic acid (HNCO) and water (H_2O) and their reaction to ammonia and carbon dioxide on the anatase phase of TiO_2 were studied with *ab initio* density functional theory (DFT) calculations using a cluster model as well as with *in situ* DRIFTS investigations and kinetic experiments. We found that isocyanic acid can in principle adsorb both molecularly and dissociatively on the TiO_2(1 0 1) surface, but the moment at which water gets involved in the process, is vital for determining the further course of the surface reaction. In the absence of water, it was found that HNCO can adsorb in molecular form on the TiO_2 surface. Assuming this case to be the first step of the HNCO hydrolysis, the surface HNCO rearranges into an intermediate complex with a modified N=C=O skeleton. After decarboxylation water attacks the complex from the gas phase and ammonia is finally formed.

However, when water is present at the beginning of the hydrolysis reaction, it immediately attacks the −NCO group present at the surface, yielding a carbamic acid complex, which is further transformed into a carbamate complex. After decarboxylation an NH_2 group remains at the surface. Finally, NH_3 is formed by hydrogen transfer from molecularly adsorbed water at a neighboring titanium center and the hydrolysis reaction is completed.

Since water is always present in diesel exhaust gas, only the second mechanism is relevant under practical conditions. Moreover, the calculated energy barrier is lower for the second mechanism compared to the first reaction pathway. The comparison between the sum of the theoretical vibrational spectra of the reaction intermediates with the *in situ* DRIFT spectra also strongly supports the accuracy of the second reaction pathway. The experimental investigation of the kinetics of the HNCO hydrolysis on TiO_2-anatase revealed a second order reaction—first order with respect to HNCO and first order with respect to water, which can only be reconciled with the second mechanism.

Keywords: Titanium dioxide; TiO_2(1 0 1) surface; Anatase structure; DFT; *In situ* DRIFTS; Cluster model; Isocyanic acid; Carbamic acid; Carbamate group

1. Introduction

A few years ago heavy-duty diesel vehicles started of being equipped with urea–SCR systems, in which the nitrogen oxides emitted by the engine are selectively reduced with urea over a catalyst. Driven by emission legislations, an ever-growing number of diesel trucks now use this process for NO_x reduction, which might also be the technical solution for passenger cars in the future.

When urea is injected into the hot exhaust gas in this process, it thermolyses to isocyanic acid (HNCO) and ammonia [1,2]:

$$NH_2CONH_2 \rightarrow HNCO + NH_3 \quad (1)$$

HNCO is a very reactive compound which can easily react with urea to biuret or trimerize to cyanuric acid (1,3,5-triazine-2,4,6-triol) [3,4]. Fortunately, these undesired reaction products can be avoided by rapid hydrolysis of the HNCO to ammonia and carbon dioxide over a broad variety of single metal oxides as well as SCR catalysts, such as V_2O_5/WO_3–TiO_2 or Fe-ZSM5. Since specialized metal oxides are more efficient for the hydrolysis than SCR catalysts, it was proposed to utilize a tailored hydrolysis catalyst in front of the SCR catalyst to overcome the problem of HNCO accumulation and to increase the efficiency of the SCR catalyst, which is optimized for the reduction of NO_x,

* Corresponding author at: Department General Energy, Paul Scherrer Institute, 5232 Villigen PSI, Switzerland. Tel.: +41 56 310 4464; fax: +41 56 310 2199.
E-mail address: izabela.czekaj@psi.ch (I. Czekaj).

1381-1169/$ – see front matter © 2007 Elsevier B.V. All rights reserved.
doi:10.1016/j.molcata.2007.10.027

but not for HNCO conversion. TiO_2 in the anatase phase, which was intensively studied during the last years [5–16], was found to be a very efficient catalyst for the hydrolysis of HNCO. In particular, the (1 0 1) surface of TiO_2-anatase is of high interest concerning reactivity and thermodynamical stability, especially under hydro treatment conditions [5,16–18].

In our previous DFT studies [19] we presented a mechanism for the hydrolysis of isocyanic acid over TiO_2-anatase (1 0 1). In this mechanism isocyanic acid adsorbs molecularly and CO_2 desorbs along with the formation of an oxygen vacancy. Then, the oxygen vacancy is covered by a water molecule and ammonia is formed, desorbing from the catalyst surface. This mechanism is indeed feasible, but based on the idealized assumption that water is not involved at the beginning of reaction. However, water is always present in diesel exhaust gas and might either alter the TiO_2(1 0 1) surface by blocking part of the titanium centers, where HNCO is expected to be adsorbed, or attack part of the –NCO surface groups, forming other reaction intermediates. Therefore, we decided to extend our previous DFT studies by calculations, in which water is present on the anatase TiO_2(1 0 1) surface right from the start of HNCO adsorption.

We started with the assumption that carbamic acid or carbamate complexes should be easily formed from the reaction between surface isocyanates and water. Kaminskaia et al. [20] have reported that carbamic acid (NH_2COOH) can be found on catalyst surfaces (e.g. palladium II) coordinated via the nitrogen atom. They have also found that NH_2COOH spontaneously decomposes into carbon dioxide and ammonia:

$$H_2N\text{-}COOH \rightarrow NH_3 + CO_2 \quad (2)$$

Interestingly enough, the backward reaction between primary or secondary amines and carbon dioxide to carbamate or carbamic acid has also been reported to be feasible, especially in aqueous systems. The potential energy surfaces and conformation preferences of NH_2COOH have been investigated using the *ab initio* molecular orbital and density functional methods by Kaur et al. [21]. Two different conformations of carbamic acid are presented: S (syn arrangement within the O–C–O–H unit) and A (anti arrangement with respect to O–C–O–H unit). The A isomer of the carbamic acid has been found to be less stable with an energy difference of ≈8.47 kcal/mol (≈0.37 eV). The molecular structure and the IR spectrum of carbamic acid were studied by Khanna et al. [22] and Wen et al. [23]. They have proposed a zwitter-ion structure with a very long C–N bond, which would result in a spontaneous decomposition into NH_3 and CO_2 already at low temperature. An *ab initio* molecular orbital method (at the 6-31G** level of theory) study of the decomposition of carbamic acid was performed by Remko and Rode [24], which also proved the easy decomposition of carbamic acid to CO_2 and NH_3. Their results show that the energy balance of reaction (2) strongly depends on the computational method. At the SCF-DFT level, which corresponds to our methodology for the study of the HNCO hydrolysis over the TiO_2-anatase surface, this reaction is endothermic and consumes ≈14.29 kJ/mol.

The objective of the present work is to study theoretically the co-adsorption and reaction of isocyanic acid and water over titania. For this purpose, the O_s–Ti_s unit of the TiO_2(1 0 1) surface has been modeled with a large molecular cluster using the density functional theory. The adsorption of water on pure TiO_2(1 0 1) and the attack of water on pre-adsorbed HNCO have been studied on this cluster and compared in detail with other theoretical predictions. We have derived possible precursors and transition states from the model calculations and developed a realistic mechanism for the HNCO hydrolysis on the TiO_2(1 0 1) surface, which is feasible under practice-relevant conditions and in accordance with the results of our catalytic experiments. In addition, theoretical infrared spectra were calculated and compared with experimental DRIFT spectra in order to identify possible reaction precursors.

2. Methods

2.1. Calculations

The tetragonal anatase phase of titanium dioxide, TiO_2, was chosen for our investigations (see details in [19]). Two different

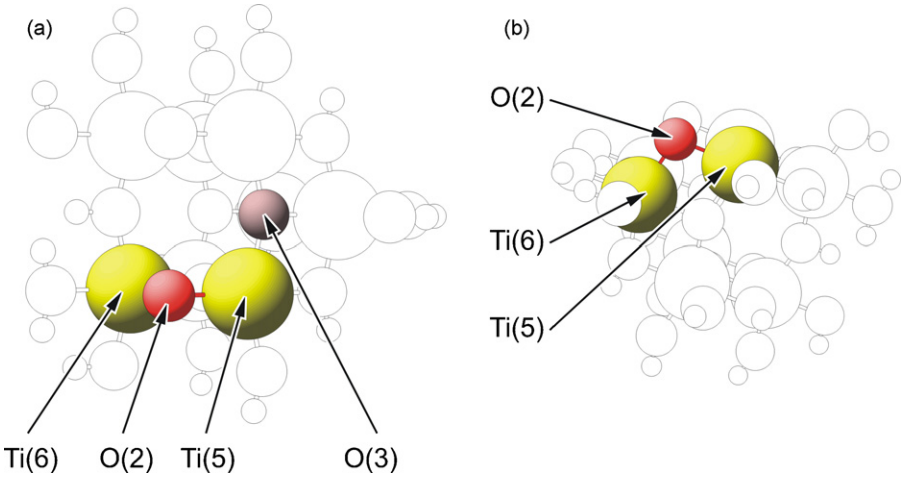

Fig. 1. $Ti_8O_{28}H_{24}$ cluster as a model for the (1 0 1) surface of the anatase phase of TiO_2 with characteristic surface as well as bulk centers: (a) top view and (b) side view. Ti (yellow) and O (red). (For interpretation of the references to colour in this figure legend, the reader is referred to the web version of the article.)

Table 1a
Main stretching band vibrations of liquid and gaseous water: comparison of experimental and theoretical vibrations

Vibration(s)	H_2O_{liquid} [36]	H_2O_{gas} [34–36]	$H_2O_{molecule}$ DFT-DZVP basis	$H_2O_{molecule}$ DFT-TZVP basis
Symmetric	2127	3657	3628 (3653)	3669 (3693)
Asymmetric	3404	3756	3788	3802

titanium sites with five- and sixfold coordinated titanium and also two different oxygen sites with two- and threefold coordinated oxygen, O(2) and O(3), can be distinguished at the TiO_2-anatase (1 0 1) surface (Fig. 1). There are two distances between the titanium centers at the (1 0 1) surface of anatase: (i) 3.78 Å between two adjacent fivefold coordinated titanium (Ti(5)) centers and (ii) 3.04 Å between an adjacent Ti(5) and Ti(6) center. The adsorbates have good access to the electrophilic Ti(5) centers, which are, therefore, preferably covered by HNCO and H_2O. Concerning the reactivity of co-adsorbed molecules, the distance between two neighboring Ti(5) centers of 3.78 Å is ideal for an atom transfer between adsorbed HNCO and adsorbed H_2O.

In our studies the TiO_2(1 0 1) surface was modeled by clusters of different size and geometry, reflecting local sections of the ideal surface. The clusters were constructed by a successive addition of neighboring shells to a small core structure. This procedure was repeated until convergence of the electronic properties of the clusters was obtained. A neutral cluster (based on formal charges: Ti^{4+}, O^{2-}) was achieved by saturating the peripheral oxygen centers with hydrogen atoms placed at the standard OH distance (R_{OH} = 0.97 Å) in the direction of the appropriate broken Ti–O bonds. In consideration of these rules, the clusters $Ti_2O_9H_{10}$, $Ti_8O_{28}H_{24}$, $Ti_{13}O_{43}H_{34}$ and $Ti_{15}O_{50}H_{40}$ were selected, among which the $Ti_8O_{28}H_{24}$ cluster proved to be best suited for the further reaction studies (Fig. 1) [19].

The electronic structure of the $Ti_8O_{28}H_{24}$ cluster and of all reaction intermediates was calculated by *ab initio* density functional theory (DFT) methods (StoBe code [25]). The generalized gradient corrected functionals according to Perdew, Burke, and Ernzerhof (RPBE) were used in order to account for electron exchange and correlation [26,27]. All Kohn–Sham orbitals are represented by linear combinations of atomic orbitals (LCAOs) using extended contracted Gaussian basis sets for the atoms [28,29]. A detailed analysis of the electronic structure of the clusters was carried out using Mulliken populations [30] and Mayer bond order indices [31,32]. In the calculations for all reaction steps, the low spin states were found to be energetically favorable.

The adsorption energies of the adsorbates on the $Ti_8O_{28}H_{24}$ cluster were calculated as follows:

$$E_{ad}(\text{adsorbate/TiO}_2) = E_{tot}(\text{adsorbate/Ti}_8\text{O}_{28}\text{H}_{24}) - E_{tot}(\text{Ti}_8\text{O}_{28}\text{H}_{24}) - E_{tot}(\text{adsorbate}),$$

where E_{tot}(adsorbate/$Ti_8O_{28}H_{24}$) is the total energy of the adsorbate/TiO_2 surface complex, E_{tot}($Ti_8O_{28}H_{24}$) and E_{tot}(adsorbate) are the total energies of pure $Ti_8O_{28}H_{24}$ and the adsorbate, respectively.

The vibration frequencies of the adsorbed molecules (e.g. water, isocyanic acid) at the (1 0 1) surface were calculated by single point energy calculations of the optimized geometries. The calculations of the vibrational frequencies were performed with harmonic approximations as well as an anharmonicity fit in the Morse potential function, as implemented into StoBe code [33]. Theoretical vibrational spectra including realistic intensities were obtained by convolution of the vibrational spectra of the individual adsorbates, applying Gaussian line-shapes. The frequencies are reported as obtained from the calculations, without scaling.

2.2. Calculations: influence of basis sets

A double zeta valence polarization (DZVP) type was used for the orbital basis sets of Ti (63321/531/41), O, C, N (621/41/1), and H (41). Auxiliary basis sets, such as (5,5:5,5) for Ti, (4,3:4,3) for O, C, N, and (41) for H, were applied to fit the electron density and the exchange-correlation potential.

In order to check the influence of a change of basis set on the computed adsorption energies and vibrational frequencies, a triple zeta valence polarization basis set of O, C, N (7111/411/1) and H (311/1), was additionally used for selected calculations.

Tables 1a and 1b show a comparison of our vibrational calculations with experimental and other theoretical data for the water molecule (Table 1a) as well as for the isocyanic acid molecule (Table 1b). A comparison of the measured wave numbers with the calculations based on harmonic and anharmonic approxima-

Table 1b
Main stretching band vibrations of isocyanic acid: comparison of experimental and theoretical vibrations

Vibration(s)	$HNCO_{gas}$ [37]	Theory-MP2 [37]	StoBe (PBE); anharmonic (harmonic)		Gaussian98 (B3LYP)
			DFT-DZVP basis	DFT-TZVP basis	
$\nu(NCO)_{sym}$	2259	2366	2259	2211	2356
$\nu(NCO)_{asym}$	1316	1310	1267 (1269)	1247 (1249)	1338
$\nu(NH)$	3511	3791	3536 (3578)	3499 (3539)	3678

tions shows that the consideration of the anharmonicity gives better results. One may wonder why the differences between the harmonic and anharmonic vibrations are small, especially for the water molecule. It is known from literature that the water molecule may vibrate in a number of ways. In the gaseous state, the vibrations [34,35] involve combinations of the symmetric stretch (υ_{sym}) and asymmetric stretch (υ_{asym}) of the covalent bonds [36]. The main stretching band in liquid water is shifted to a lower wave number (υ_{asym}, 3490 cm^{-1} and υ_{sym}, 3280 cm^{-1} [36]) by hydrogen bonding. This is due to the fact that in the liquid, rotations tend to be restricted by hydrogen bonds, resulting in librations. Also, spectral lines are broader causing overlap of many of the absorption peaks.

The obtained vibrations for the water molecule are not far away from the experimental data for gaseous water (see Table 1a) which suggests, in combination with our interpretation of the shift of the stretching vibrations due to hydrogen bonding, that our computations are correct as well as that the DZVP basis sets are sufficient for the interpretation of the DRIFTS experimental data. Results of our calculations for pure isocyanic acid are included (Table 1b) to show that also in this case our calculations agree with other experimentally found vibrations. Based on these results we assume that also in case of adsorbate–surface complexes vibrational frequencies would be reasonably represented by DZVP basis sets. In fact, the adsorption energies of the water molecule calculated with the DZVP and the TZVP basis sets were found to be very similar (see Table 2, Section 3.1).

2.3. Experiments

TiO_2-anatase with a surface area of 57 m^2/g was used for the experiments. Isocyanic acid was produced by thermal decomposition of cyanuric acid as described in [1] and mixed with the feed gas.

In situ diffuse reflectance infrared Fourier transform spectroscopy (DRIFTS) was performed on a Thermo Nicolet Nexus 860 FT-IR spectrometer. The catalyst sample was pre-treated *in situ* for 1 h at 450 °C with a flow of N_2. All spectra were collected with 200 scans and a resolution of 4 cm^{-1}. Isocyanic acid adsorption was studied from room temperature to 450 °C by treating the catalyst with ≈70 ppm of HNCO in N_2 for 15 min. Then the catalyst was degassed in a N_2 flow for 15 min before water was injected in pulses through a capillary.

Basic kinetic investigations were carried out in a differential micro-plug flow reactor in order to determine the reaction orders for the different reactants and products in the power-law rate equation of the HNCO conversion:

$$r_{HNCO} = -k_a[HNCO]^{\alpha}[H_2O]^{\beta}[NH_3]^{\chi}[CO_2]^{\delta}$$

The initial concentration of each component was systematically varied, thereby over-supplying the other components, which can be considered as constant. The reaction orders were then determined from the slope of the logarithm of the reaction rate plotted as a function of the logarithm of the component concentration. Please note that the selectivity to NH_3 was always 100% ($S_{NH_3} = 100\%$). Thus, either the conversion of HNCO (X_{HNCO}) or the yield of NH_3 (Y_{NH_3}) can be used for the evaluation of the experiments.

Due to the very high reaction rates, minimal amounts of TiO_2 (50 mg) were used, which were additionally diluted in 100 mg of SiC (particle size 160–200 μm), in order to keep the conversion below 30%.

Several tests performed with CO_2 showed that carbon dioxide had no influence on the measured reaction rates. Therefore, CO_2 was omitted in the following kinetic experiments. The flow rate was kept constant at 300 l_N/h for all experiments.

For determining the reaction order with respect to NH_3 (δ), the concentrations of HNCO and H_2O were kept constant at 1000 ppm and 2.5%, respectively, while the concentration of NH_3 was varied from 200 to 1000 ppm. For determining the reaction order with respect to HNCO (α), the concentration of H_2O was kept constant at 2.5%, while the concentration of HNCO was varied from 400 to 1000 ppm. In consideration of the found reaction order for ammonia ($\delta = 0$ for $T > 150$ °C) no ammonia was dosed. This also reduced the risk of by-product formation from the reaction between HNCO and NH_3. For the tests at 175 °C, the amount of TiO_2 had to be further reduced in order to keep the conversion low. Therefore, 25 mg of catalyst were diluted in 100 mg of SiC. For determining the reaction order of water (β), the HNCO inlet concentration was ∼1000 ppm, while the concentration of H_2O was varied from 150 to 1000 ppm.

Table 2
Comparison of the adsorption energies for water on the TiO_2(1 0 1) surface

Reference	Method	Surface representation	Adsorption energy (eV)	
			Molecular ads.	Dissociative ads.
This work	DFT-GGA (RPBE) DZVP (TZVP)	$Ti_8O_{28}H_{24}$ cluster relaxed	−1.19 (−1.16)	−0.84 (−0.85)
Onal et al. [38]	DFT B3LYP/6-31G**	$Ti_2O_9H_{10}$ cluster relaxed/ideal	−1.09/−1.26	−0.83/−1.51
Vittadini et al. [39]	DFT-GGA (PW91)	Slab	−0.72 ($\theta = 1$)[a]	−0.40 ($\theta = 1$)
			−0.74 ($\theta = 0.25$)	−0.23/−0.30 ($\theta = 0.25$)
Selloni et al. [40]	Molecular dynamics	101 Anatase	−0.75	−0.30/−0.38
Tilocca at al. [41]	DFT-GGA (PBE)	Slab, defected surface (O_{vac})	−0.60	
			$-1.20/-1.48_{(at\ Ovac)}$	-1.49 to $-1.86_{(at\ Ovac)}$
Redfern et al. [42]	B3LYP/6-31G*//B3LYP/6-31G*	$Ti_6O_{22}H_{20}$ cluster	−1.18/−1.15	−0.86/−0.68
Arrouvel et al. [5]	DFT-GGA (PW91)	Slab	−0.72	–

[a] θ is the surface coverage of the (1 0 1) surface with water.

3. Results

3.1. Water adsorption at TiO_2(1 0 1)

Water adsorption at TiO_2(1 0 1) was considered, due to its high importance, for the hydrolysis of isocyanic acid. Molecular as well as dissociative adsorption of water was found to be feasible on the TiO_2(1 0 1) surface. Fig. 2 shows the geometric and the electronic structures for both types of adsorption. Although water is bonded to the Ti(5) center via the oxygen in both cases, the Ti(5)–OH_2 distance and bond strength depend on the type of adsorption, as depicted in Fig. 2b and c. In the event of dissociative adsorption (Fig. 2c) one hydrogen atom of the water molecule is transferred and stabilized at the neighboring O(2) center of the (1 0 1) surface. As a consequence the entire surface including the O(2) centers is covered by hydroxyl groups. It is important to note that the bonds of the O(2) centers with the surface are weakened by ≈50% due to formation of the OH groups.

The adsorption of water on the (1 0 1) surface of TiO_2-anatase was already investigated in several theoretical studies [5,38–42], which are compared with our DFT calculations in Table 2. The calculations with a relaxed $Ti_8O_{28}H_{24}$ cluster show that molecular adsorption of water is more favorable ($E_{ad} = -1.19$ eV) than dissociative adsorption ($E_{ad} = -0.84$ eV). All studies, which took the relaxation of the neighboring centers at the TiO_2(1 0 1) surface into account, agreed on the conclusion that molecular adsorption of water is more favorable than dissociative adsorption. Alongside the consideration of the neighboring centers, the size of the cluster model also has a major influence on the accuracy of the calculations. As previously shown in [19], the $Ti_8O_{28}H_{24}$ cluster is a good representation for the electronic states of the TiO_2(1 0 1) surface. Our results of water adsorption at $Ti_8O_{28}H_{24}$ (Table 2) agree with the results obtained by Onal et al. [38] and Redfern et al. [42], who used a $Ti_2O_9H_{10}$ and a $Ti_6O_{22}H_{20}$ cluster, respectively, for both types of water adsorption. However, small mismatches in the adsorption energies are observed compared with the values of Onal et al. [38], which are likely due to the relatively small $Ti_2O_9H_{10}$ cluster with only two titanium centers, used in their work.

Deeper insight into the details of water adsorption at the TiO_2 surface was provided by DRIFTS experiments and a comparison of the obtained spectra with calculated vibrational frequencies. We were particularly interested in changes of the water population at the TiO_2 surface before and after drying of the catalyst at higher temperatures.

Fig. 3 shows that the band at 1629 cm^{-1} found in the DRIFT spectrum at 50 °C is in good agreement with the vibrational frequency 1646 cm^{-1} obtained from DFT calculations for molecularly adsorbed water. There is also a fair match between the band at 3691 cm^{-1} in the DRIFT spectrum and the band at 3744 cm^{-1} in the DFT spectrum. On first view it seems that the band at 3630 cm^{-1} is also caused by molecularly adsorbed water. However, this band is more likely to be caused by dissociatively adsorbed HNCO with the theoretical value 3623 cm^{-1}. The bands at 3670/3667 cm^{-1} in the DRIFT spectra at 50 and 450 °C, respectively, are also compatible with dissociatively adsorbed water with a calculated band at 3654 cm^{-1}. The

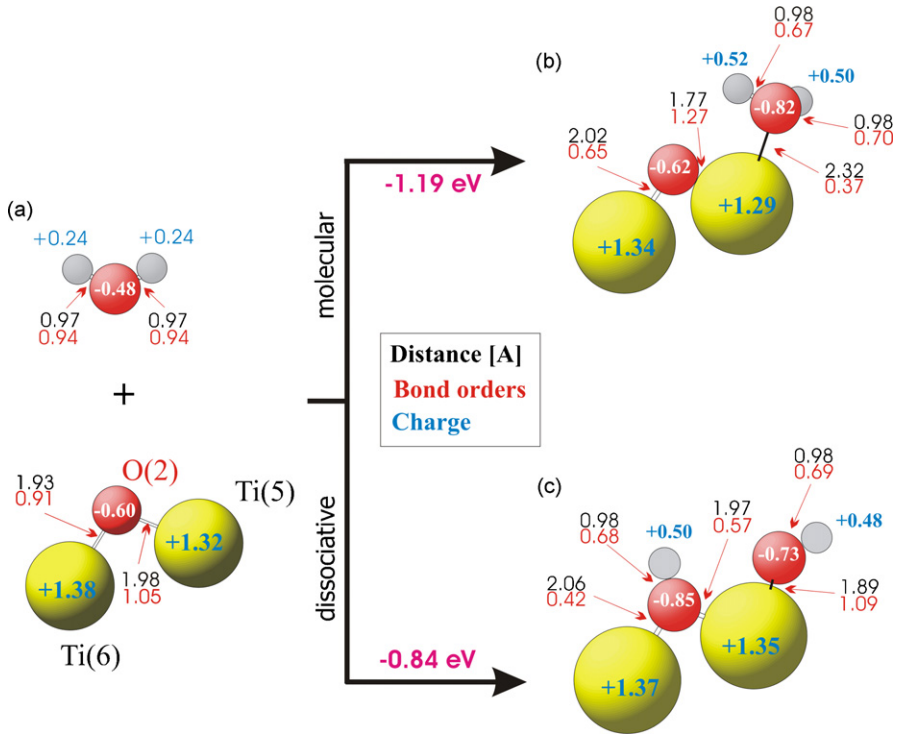

Fig. 2. Water adsorption at the $Ti_8O_{28}H_{24}$ model cluster. (a) Water and the interacting sites at $Ti_8O_{28}H_{24}$. (b) Molecular water adsorption at $Ti_8O_{28}H_{24}$. (c) Dissociative water adsorption at $Ti_8O_{28}H_{24}$. Ti (yellow) and O (red), H of water (gray). (For interpretation of the references to colour in this figure legend, the reader is referred to the web version of the article.)

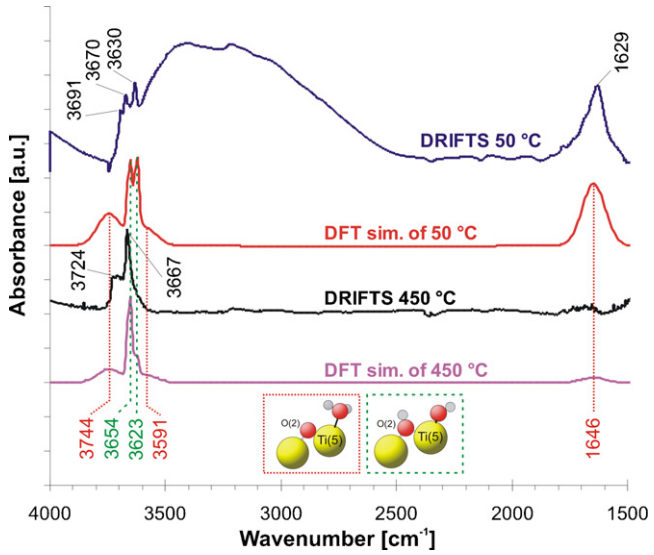

Fig. 3. Theoretical vibrational IR spectra and experimental DRIFT spectra of fresh TiO_2. (a) DRIFT spectrum at 50 °C. (b) Theoretical IR spectrum at 50 °C. (c) DRIFT spectrum at 450 °C. (d) Theoretical IR spectrum at 450 °C. Vertical lines correspond to calculated wave numbers for (1) molecular adsorption of water at $Ti_8O_{28}H_{24}$ (red dotted line), and (2) dissociative adsorption of water at $Ti_8O_{28}H_{24}$ (green dashed line). (For interpretation of the references to colour in this figure legend, the reader is referred to the web version of the article.)

stretching vibration at 3623 cm^{-1} is connected with hydroxyl groups adsorbed at the Ti(5) centers and the stretching vibration at 3654 cm^{-1} results from hydroxyl groups formed with the $O_s(2)$ surface oxygen atoms ($O_s(2)$–H). However, the detailed analysis of the experimental spectra at 450 °C shows that the absorbance of the Ti(5)–OH vibration is much weaker than that of $O_s(2)$–H, which suggests a higher population of $O_s(2)$–H. A lower population of hydroxyl groups at Ti(5) centers is a very important feature for the adsorption of HNCO on these sites as a prerequisite for the hydrolysis reaction. Please note that the DRIFT spectrum of TiO_2 at 50 °C shows also a broad band in the range 2500–3740 cm^{-1}, which is typical for the presence of liquid water due to strong hydrogen bonds (see Table 1a) [34–36,43].

The comparison of the calculated vibration frequencies with the DRIFTS experiments suggests that at lower temperatures (50 °C) both molecular (1629 and 3630 cm^{-1}) and dissociative (3670 and 3691 cm^{-1}) adsorption occur with slightly higher amounts of molecular water. At higher temperatures (450 °C) mainly dissociative adsorption (3667 and 3724 cm^{-1}) was observed. The asymmetry in the peak at 3667 cm^{-1} towards lower wave numbers in the DRIFT spectrum at higher temperature (450 °C) as well as the weak band at ~3740 cm^{-1} suggest that some water still exists in molecular form at the TiO_2 surface. However, its concentration is negligible after drying of the catalyst at 450 °C and most of the weak hydrogen bonding between water molecules, which was observed at lower temperature and which is characteristic for liquid water, is not observed due to water molecules separation at the surface.

3.2. *Surface adsorbates upon coadsorption of isocyanic acid and water*

Dissociative as well as molecular adsorption of HNCO is possible and energetically feasible on the TiO_2(1 0 1) surface [19]. Fig. 4 shows the geometric and electronic structures of HNCO and the important intermediates in the reaction path (e.g. NH_2COOH, NH_2CO_2) as well as the interacting sites of TiO_2(1 0 1), represented by the $Ti_8O_{28}H_{24}$ cluster (see Fig. 1). Information about atomic charges (Mulliken analysis; blue), distances (Å) (black) and bond orders (Mayer bond analysis; red) are also included.

The mechanism with an early influence of water proceeds via dissociative adsorption of HNCO at the TiO_2(1 0 1) surface. Adsorption of HNCO is actually possible in the presence of water, because the dissociative adsorption of HNCO is energetically competitive to the dissociative adsorption of water

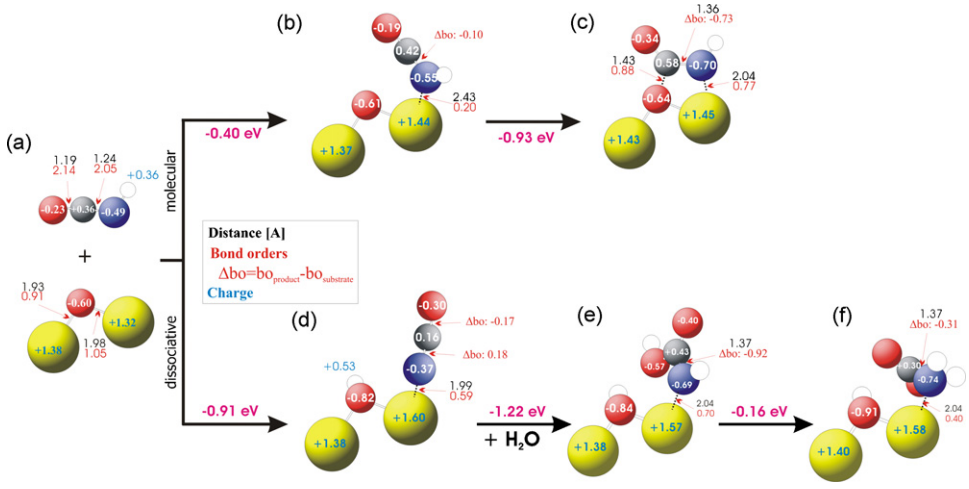

Fig. 4. Isocyanic acid adsorption on the $Ti_8O_{28}H_{24}$ cluster: electronic structures including atomic charges (Mulliken analysis), distances (Å) and bond orders (Mayer bond analysis). (a) Gaseous HNCO and the interacting sites at TiO_2. (b) Molecular adsorption of HNCO. (c) The intermediate complex HNCO/TiO_2. (d) Dissociative adsorption of HNCO. (e) The surface complex of carbamic acid (NHCOOH) at a Ti(5) site. (f) The carbamate (NH_2CO_2) complex at a Ti(5) site.

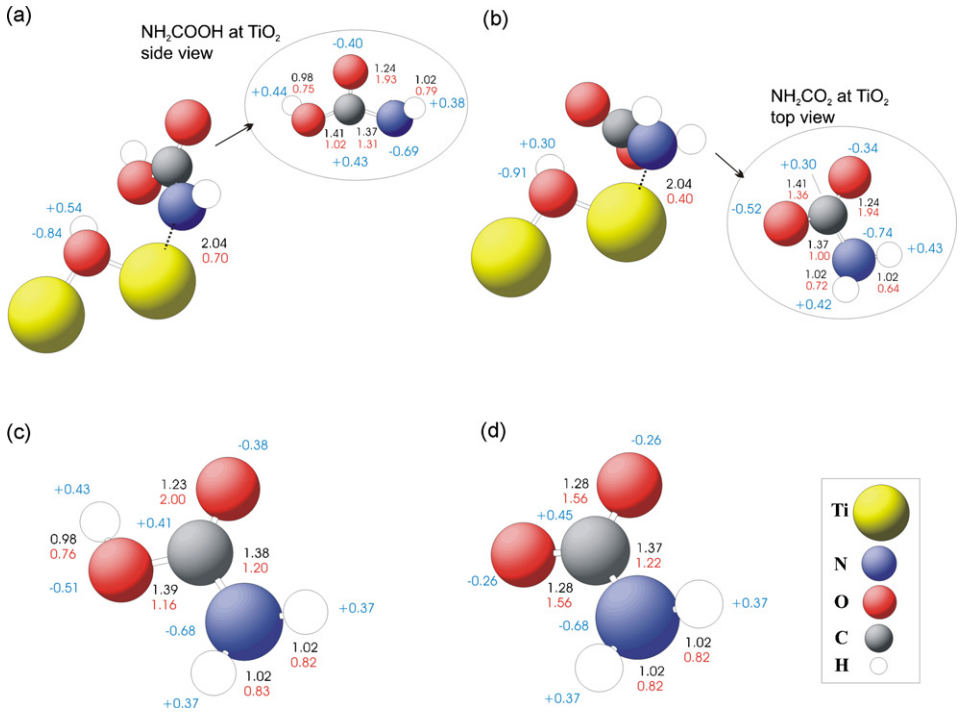

Fig. 5. Carbamic acid and carbamate on the $Ti_8O_{28}H_{24}$ cluster: electronic structures including atomic charges (Mulliken analysis), distances (Å) and bond orders (Mayer bond analysis). (a) Carbamic acid (NHCOOH) at a Ti(5) site. (b) The carbamate (NH_2CO_2) complex at a Ti(5) site. (c) Gaseous carb acid (NH_2COOH). (d) Unbonded carbamate (NH_2CO_2).

on the TiO_2 surface. The –NCO group is stabilized at a Ti(5) center with an adsorption energy of −0.91 eV (see Fig. 4d) [19], whereas water adsorbs dissociatively with an adsorption energy of E_{ad} = −0.84 eV (see Section 3.1). Although molecular adsorption of water should be energetically even more favored (E_{ad} = −1.19 eV), dissociative adsorption of water is observed over the whole temperature range and even at very low temperatures (50 °C). Following our result of a lower population of the terminal hydroxyl groups, there is always a sufficiently high number of Ti(5) sites available for the dissociative adsorption of HNCO to –NCO groups.

In the next step of the mechanism, a water molecule from the gas phase attacks the –NCO group. A strong interaction of water with the C–N couple is observed, leading to an –NCO skeleton transformation and the formation of a carbamic acid complex with an S (syn) arrangement within the O–C–O–H unit (Fig. 4e). The carbamic acid is bound with an adsorption energy of −2.13 eV (−49.1 kcal/mol; −1.22 eV with respect to adsorbed –NCO) along with a weakening of the N–C bond by −0.9 Δ bond order units (see Fig. 4e).

To conclude, it can be pointed out that the formation of the surface bound carbamic acid proceeds immediately and without an energy barrier after the attack of the –NCO group by a water molecule. The surface carbamic acid (–NHCOOH) is connected with a Ti(5) center by an almost single bonded nitrogen (see Fig. 5a) and has an electronic structure similar to gaseous carbamic acid (see Fig. 5c as well as [21–23]). Bond distances of ∼1.23 Å for C=O, ∼1.38 Å for C–N, and ∼1.39 Å for C–O_{OH} were calculated for the gaseous carbamic acid (Fig. 5c) corresponding to the values of Kaur et al. [21].

By a change of the "S" conformation of the O–C–O–H unit to the "A" conformation of the surface bound carbamic acid (see Fig. 10c–g, next Section 4.1) a carbamate complex can be formed at the surface (see Figs. 4f and 5b). The carbamate complex is weakly bonded at the Ti(5) center via nitrogen (∼0.4 bond order

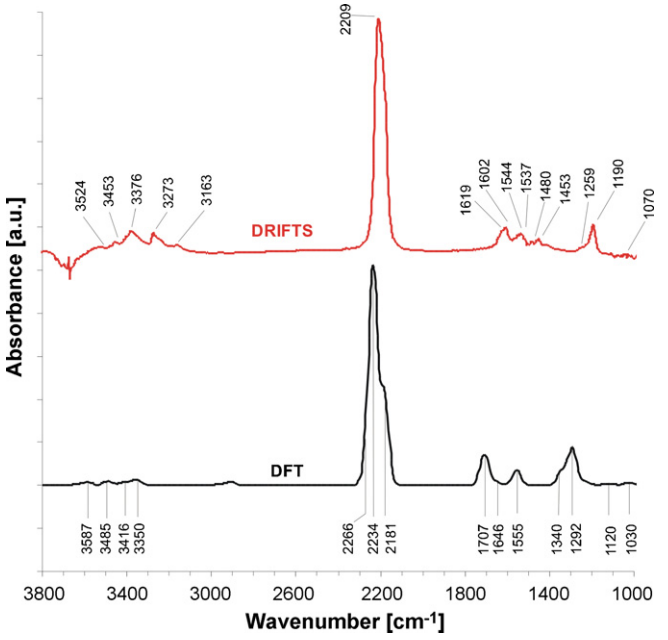

Fig. 6. Theoretical vibrational IR spectra and experimental DRIFT spectra of TiO_2 after HNCO adsorption (70 ppm) at 150 °C for 15 min followed by purging with nitrogen for 15 min.

units) with an adsorption energy of −2.29 eV (−52.9 kcal/mol; −0.16 eV with respect to the adsorbed "S" carbamic acid level). The adsorbed carbamate complex has a similar geometrical structure as the gaseous complex (see Fig. 5d) with exception of the C–N bond. This bond is about 0.22 bond order units weaker than in the gaseous complex, which is important for the HNCO hydrolysis reaction. The adsorbed carbamate complex (Fig. 5b) has a more ionic character than the gaseous complex (see Fig. 5d) with a total charge of about −0.45, which would result in a spontaneous decomposition into NH_3 and CO_2 even at low temperature. The calculated geometric structure of the surface carbamate ion (Fig. 4d) with distances of ∼1.25 Å for C=O, ∼1.43 Å for C–N, and ∼0.99 Å for C–O_{OH} differs only slightly from that obtained by Wen et al. [23].

Fig. 6 compares the DRIFT spectrum after HNCO adsorption at 150 °C with the theoretical vibrational spectrum of the individual adsorbates at TiO_2(1 0 1) surface. The theoretical spectrum was obtained by summation of the spectra of the individual adsorbates such as ammonia, carbamic acid and isocyanic acid as well as amino, carbamate, and isocyanate groups, each influenced by an aqueous environment in form of H_2O or OH groups. Additionally, the theoretical vibrational frequencies of the individual adsorbates at the TiO_2(1 0 1) surface are listed in Table 3. From the comparison of the anharmonic vibrational frequencies with its harmonic approximations it is obvious that there is almost no deviation between these values, except for the motion of H atoms and its bonds, which is consistent with previous findings of Leviel et al. [44].

Exposure of the catalyst to HNCO at 150 °C resulted in the evolution of a strong band at 2209 cm^{-1} together with less intense bands in the range 3524–3163 and 1619–1190 cm^{-1} (see upper spectrum in Fig. 6). The strong band at 2209 cm^{-1} is assigned to the asymmetric stretching vibrations of –NCO groups adsorbed at the surface. From our theoretical studies we found that the main contributions to these vibrations come from dissociatively adsorbed isocyanic acid stabilized at a Ti(5) center (see Fig. 7) evoking the vibration at 2234 cm^{-1} in the neighborhood of strong OH groups and the vibration at 2181 cm^{-1} in the absence of OH group. However, small amount of weakly adsorbed HNCO in molecular form can be found at 2266 cm^{-1}, which is very close to the vibration of gaseous HNCO. Our theoretically predicted vibrations are consistent with results of Hauck et al. [45], who recorded transmission IR spectra of the HNCO adsorption on the same TiO_2-anatase catalyst at 120 °C and who found a more significant asymmetry in this band with components at 2189, 2230 and 2255 cm^{-1}. The calculated bands below 1800 cm^{-1} and above 3000 cm^{-1} in Fig. 6 have a similar shape like in the experimental spectrum, but they are slightly

Table 3
Theoretical vibrational frequencies (cm^{-1}) of individual surface intermediates on the TiO_2(1 0 1) surface, represented by a $Ti_8O_{28}H_{24}$ cluster

Vibration mode	NHCOOH[a]	NH_2CO_2[b]	NH_{2aq}[c]	NH_{3aq}[d]	NH_3[e]
	Anharmonic (harmonic) frequency (cm^{-1})				
(a)					
N–H and/or O–H, bending	1137	1030	–		
	1266 (1267)	1099			
	1329	1231		1334	1292
H–N–H bending	–	1588	1555	1646	1654
N–H and/or C=O bending	1716 (1718)	1703		1704	1687
N–H sym. stretching	3462 (3499)	–	–	2955	3114 (3125)
H–N–H sym. stretching	–	3346 (3368)	3349 (3359)	3381 (3414)	3415 (3421)
H–N–H asym. stretching	–	3482	3466	3485 (3492)	3496 (3498)

Vibration mode	H_2O_{mol}[f]	H_2O_{diss}[g]	NCO_{aq}[h]	NCO[i]	HNCO[j]	$HNCO_g$[k]
	Frequency (cm^{-1})					
(b)						
H–O–H bending	1646	–	–	–	–	–
N–H or OH stretching	3591 (3614)	3623 (3667)	–	–	3281 (3324)	3526 (3578)
	3744 (3746)	3654 (3702)				
NCO sym. stretching	–	–	1351 (1352)	1345	1279	1269
NCO asym. stretching	–	–	2234	2181	2266 (2267)	2259

[a] Carbamic acid (see Fig. 4e and Fig. 10c).
[b] Carbamic complex (see Fig. 4f and Fig. 10g).
[c] NH_2 at Ti(5) influenced by H_2O at neighbored Ti(5) and by OH at O(2) (see Fig. 10k).
[d] NH_3 at Ti(5) influenced by OH at neighbored Ti(5) and by OH at O(2) (see Fig. 10l and m).
[e] NH_3 at Ti(5) (see Fig. 10j).
[f] Molecularly adsorbed H_2O (see Fig. 2b).
[g] Dissociatively adsorbed H_2O (see Fig. 2c).
[h] NCO at Ti(5) influenced by OH at O(2) (see Fig. 10b).
[i] NCO at Ti(5) (see Fig. 7).
[j] HNCO molecularly adsorbed at Ti(5) (see Fig. 4b)
[k] HNCO molecule in gas phase.

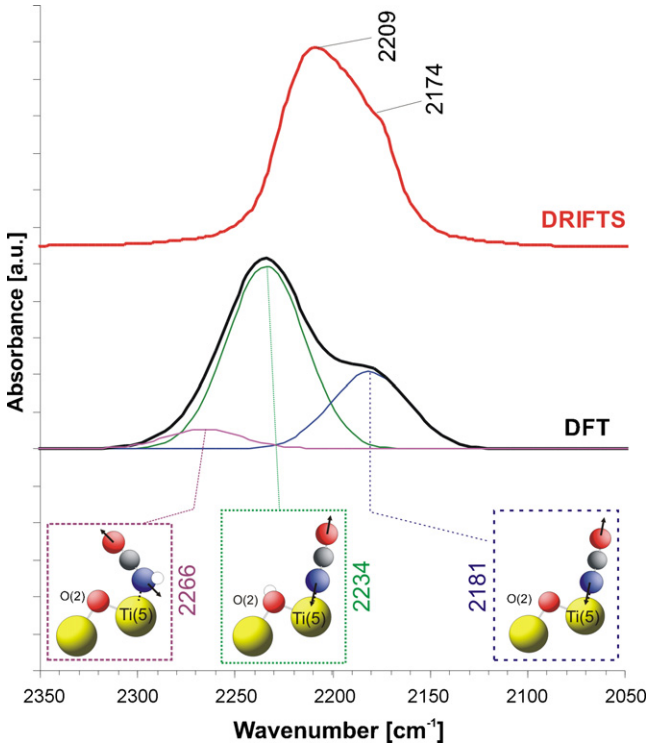

Fig. 7. The bands typical for adsorbed isocyanate species are shown in detail in an enlarged view of the region 2050–2350 cm^{-1} in Fig. 6.

shifted to higher wave numbers, which could originate from the fact that only adsorbates were added which are directly involved in the isocyanic acid hydrolysis without including other parallel reaction paths. Both of the referred bands are strongly influenced by water at the surface and by side-reactions, such as the dimerization or trimerization of isocyanic acid. Despite these small deviations, the calculated IR spectra can help to gain a deeper understanding of the mechanism of the HNCO hydrolysis, especially of the role of water. The bands below 1800 cm^{-1} in the calculated spectrum in Fig. 6 and Table 3 are composed of the bending vibrations of NH_2 or NH_3 groups influenced by water as well as NH_2CO_2 and NHCOOH and the symmetric stretching vibrations of NCO influenced by water. Hauck et al. [45] tentatively attributed the bands in region 1810–1429 cm^{-1} to different species co-existing on the surface after HNCO adsorption and hydrolysis as well as to different possible side-products formed (e.g. urea, cyanuric acid, melamine or cyanamide). Our DFT calculations of the vibrational frequencies of the different possible reaction intermediates (Figs. 4 and 5) indicate three regions in Fig. 6: (i) the band at 1707 cm^{-1} is assigned to surface coordinated complexes, mainly NH_2COOH and NH_{2aq} with a small contribution of NHCOOH; (ii) the band at 1646 cm^{-1} is attributed mainly to ammonia, and (iii) the band at 1555 cm^{-1} is caused by surface amino groups, NH_{2aq}. In addition, the band at 1292 cm^{-1} can be assigned to N–H bond vibrations, mainly from the ammonia bending mode with a small contribution from the NH_2CO_2 scissor mode and from the –NCO symmetric stretching mode.

The peaks above ~3000 cm^{-1} of the calculated spectrum corresponds to the N–H stretching vibrations of the individual adsorbates (see Table 3), which are strongly influenced by neighbored O–H vibrations. However, the negative band at ~3700 cm^{-1} in the differential DRIFT spectrum indicates the consumption of water or hydroxyl groups and therefore suggests a deficiency of OH groups at the surface during reaction. The remaining differences between our experimental and theoretical vibrational spectra, especially in region 1400–1500 cm^{-1} as well as region 3100–3300 cm^{-1} might be assigned to different species co-existing on the surface after HNCO adsorption and their polymerization as it was suggested by Hauck et al. [45]. A theoretical study is running in our laboratory in order to identify these species, which can appear during HNCO adsorption on TiO_2.

3.3. Reaction orders for HNCO, H_2O, NH_3 and CO_2 in the HNCO hydrolysis

A helpful method to prove or disprove a proposed mechanism is to check the kinetics of the reaction. The found reaction orders for the different components of the reaction network must be in agreement with the energy barriers of the mechanism. For instance, when two reactants are involved in the reaction steps before the first major energy barrier the experimentally found reaction orders should be >0 for these two components.

Several tests performed with CO_2 showed that carbon dioxide had no influence on the reaction rate, indicating that the CO_2 reaction order is 0. The experimental results for the rate of HNCO consumption as a function of the ammonia inlet concentration from 125 to 150 °C are presented in Fig. 8a. For each data set, the coefficient of determination, R^2, exhibits a good linear fit between the reaction rate and reactants' concentration. It is interesting to note that the rate of reaction measured at 125 and 135 °C decreases slightly for increasing NH_3 concentration, revealing an 'inhibition effect' of ammonia, due to the adsorption of ammonia on the catalyst surface. This inhibition becomes more significant at lower temperatures, where ammonia adsorption is favored. However, for $T = 150$ °C this effect became very small and the reaction rate remained constant. From the slope of the regression line, activation orders of 0.29, 0.16 and 0.08 were obtained at 125, 135 and 150 °C, respectively. An additional test performed at 175 °C with 25 mg of TiO_2 (bed of 150 mg total) showed that the influence of NH_3 on the reaction rate is further reduced at this temperature. This leads to the conclusion that the reaction order of NH_3 can be approximated as 0 for $T > 150$ °C. The rate of HNCO consumption is shown as a function of the HNCO concentration in Fig. 8b. The coefficient of determination, R^2, shows an excellent linear fit. From the slope of the regression curves, activation orders of 0.92 and 0.97 were obtained at 175 and 150 °C, respectively. The experimental results of the determination of the reaction order of water (β) are depicted in Fig. 8c. The coefficient of determination, R^2, shows an excellent linear fit. From the slopes of the regression lines, activation orders of 1.09 were obtained at 175 and 150 °C. For typical diesel exhaust conditions, i.e. in the presence of excess of water, H_2O showed only negligible influence on the reaction. This indicates that in this case the surface of TiO_2 is covered

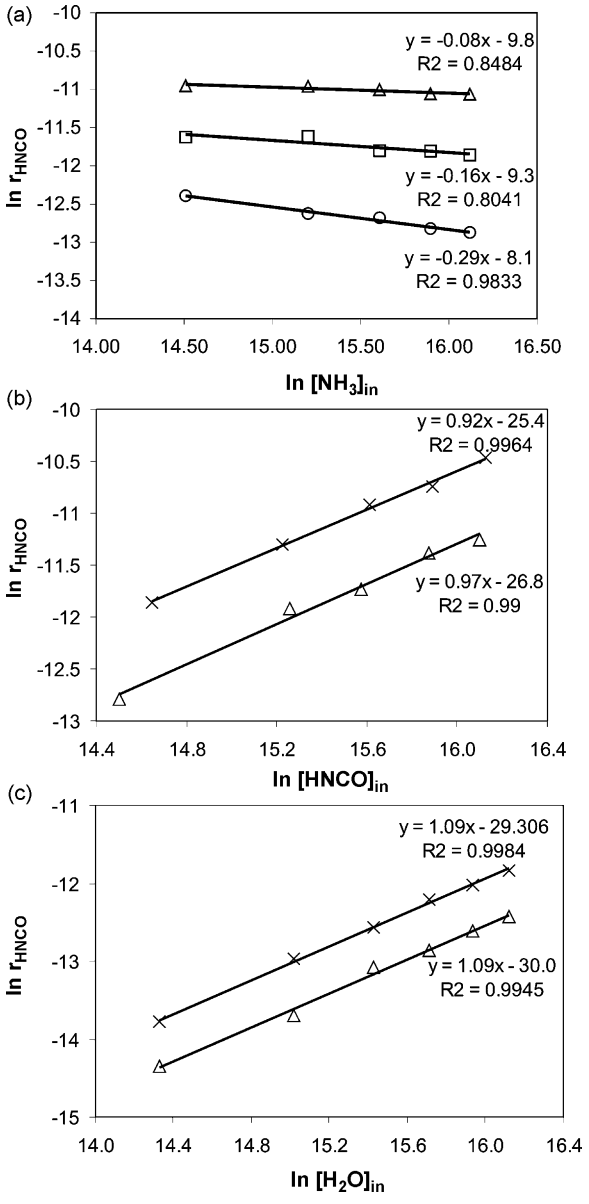

Fig. 8. Logarithmic plots of the measured reaction rate as function of the (a) NH_3, (b) HNCO, and (c) H_2O inlet concentration. (a) 50 mg, (b) 25 mg, and (c) 50 mg of TiO_2. (◯) 125 °C, (□) 135 °C, (△) 150 °C, and (×) 175 °C.

with water and that the reaction order β can be approximated as 0.

4. Discussion

4.1. Reaction path of HNCO hydrolysis with early influence of water

Based on the results of the calculations, a probable reaction pathway was developed for the hydrolysis of HNCO over the (1 0 1) surface of the anatase phase of TiO_2, with water getting involved at an early stage of the reaction (Fig. 9). The proposed reaction mechanism considers co-adsorption of HNCO and H_2O at the surface and involves mainly five-fold coordinated titanium sites. Co-adsorption means either

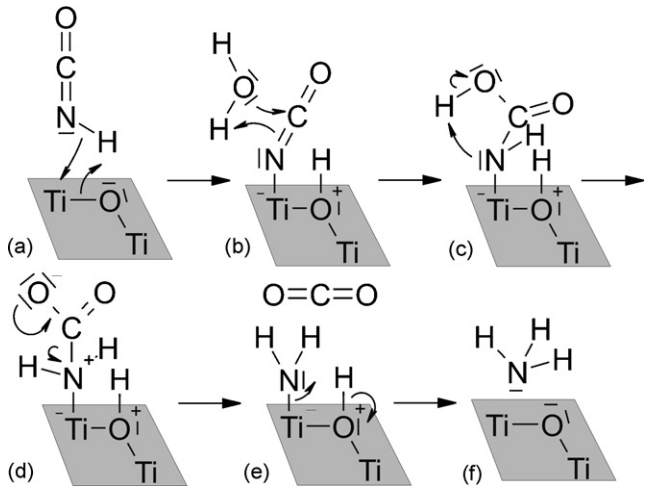

Fig. 9. The reaction pathway for the hydrolysis of HNCO over the (1 0 1) surface of TiO_2 in the presence of water at the beginning of the mechanism. (a) Dissociative adsorption of HNCO. (b) Water attack to an –NCO group. (c) Formation of carbamic acid. (d) Formation of a carbamate complex. (e) CO_2 desorption. (f) Formation of NH_3.

that there is competitive adsorption between water and isocyanic acid at Ti(5) centers (see Section 3.1) or that water interacts with the isocyanic acid adsorbates, leading to the formation of carbamic acid and carbamate complexes at the surface (see Section 3.2). Since competitive adsorption of water at the Ti(5) centers will limit the hydrolysis of HNCO, which was not observed in the catalytic tests [1], this option was abandoned and only the reaction of water with adsorbed isocyanic acid needs to be considered in the mechanism.

In the first step isocyanic acid dissociates on the surface ($HNCO \rightarrow H^+ + NCO^-$), in such a way that the proton adsorbs at an $O(2)_s$ site and the NCO^- anion at a $Ti(5)_s$ site (Fig. 9a). Subsequently, the –NCO group is attacked by water from the gas phase (Fig. 9b), which results in the immediate formation of a more stable carbamic acid adsorbate (–NHCOOH, Fig. 9c). After internal hydrogen transfer from the carboxyl group to the nitrogen, a carbamate adsorbate ($–NH_2CO_2$) is formed (Fig. 9d), from which CO_2 is desorbed (Fig. 9e). The hydrogen atom from the surface $O(2)_sH$ group reacts with the remaining $–NH_2$ group at the $Ti(5)_s$ site forming an ammonia molecule, which successively desorbs from the surface (Fig. 9f).

The results of the energy calculations are summarized in Fig. 10 for each step of the proposed reaction mechanism. In the energy diagram, the sum of the total energies of the $Ti_8O_{28}H_{24}$ cluster and the HNCO molecule was taken to be the reference level of zero energy (Fig. 10a).

First, the HNCO molecule adsorbs dissociatively with the proton at an $O(2)_s$ site and the NCO anion at a $Ti(5)_s$ site (see Fig. 10b), releasing an adsorption energy of about −0.91 eV. Then, a water molecule from the gas phase attacks the adsorbed isocyanate, resulting in the immediate formation of adsorbed carbamic acid (–NHCOOH). This reaction is highly exothermic with an energy balance of −2.13 eV with respect to the reference level (see Fig. 10c). After a change from the "S" to

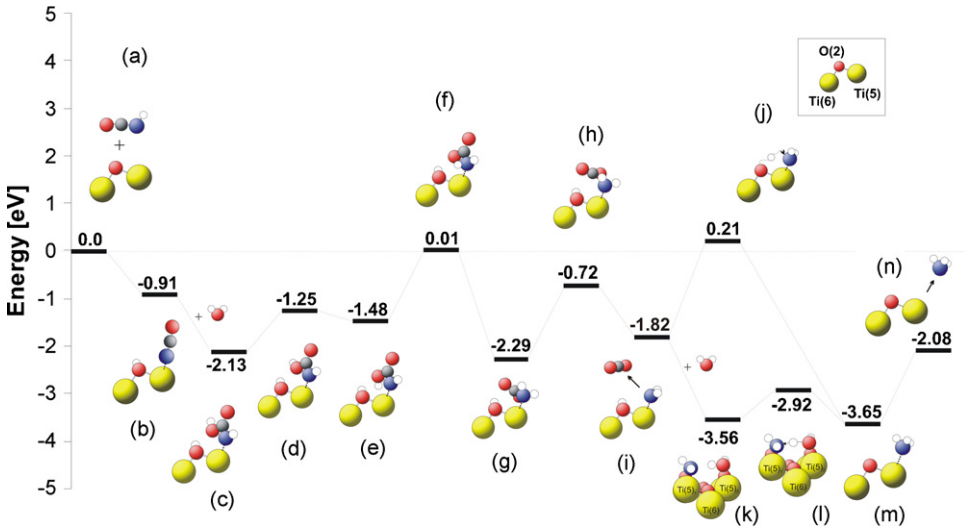

Fig. 10. Energy diagram of the reaction pathway for the hydrolysis of HNCO on the TiO_2 surface: (a) $Ti_8O_{28}H_{24}$ + HNCO reference level. (b) Dissociative adsorption of the HNCO on $Ti_8O_{28}H_{24}$. (c) Water attack to an NCO group at a Ti(5) site and formation of surface carbamic acid (NHCOOH). (d) and (e) Rotation of the H at the carboxyl group. (f) Transfer of the carboxyl H to the NH group. (g) Formation of adsorbed carbamate (NH_2CO_2) at the Ti(5) site. (h) CO_2 separation from the NH_2 surface group. (i) CO_2 desorption and stabilization of the NH_2 group at the Ti(5) site. (j) Migration of the H from the surface OH group to NH_2. (k) Molecular adsorption of water at a neighboring titanium center. (l) Migration of the H from the adsorbed water to the NH_2 group. (m) NH_3 at the Ti(5) site. (n) NH_3 desorption from TiO_2 surface.

the "A" conformer [21] (see Fig. 10c–e), the hydrogen atom at the oxygen is internally transferred to the nitrogen of the carbamic acid molecule. This process is highly endothermic with an energy barrier of about 1.49 eV (see Fig. 10f), but is directly followed by the release of −2.30 eV in the very exothermic formation of a stable carbamate complex (see Fig. 10g). Next, CO_2 is desorbed by decomposition of the carbamate complex (see Fig. 10i), and the $–NH_2$ group remains at the Ti(5) center. The hydrogen missing for the formation of ammonia can be provided in different ways. The first possibility is an internal hydrogen transfer from the hydroxyl group at the O(2) center to the NH_2 group. However, this process has an activation energy of ≈2 eV as reported in [19] (see Fig. 10j) and is, therefore, less probable. The second way to obtain an ammonia molecule is a hydrogen transfer from a water molecule adsorbed at a neighboring Ti(5) center. This mechanism is favored due to the very low energy level of the system after the adsorption of water (−3.56 eV; see Fig. 10k) and the only moderate energy barrier of 0.64 eV for the subsequent hydrogen transfer (see Fig. 10m). By the reaction of NH_2 groups with adsorbed water molecules to NH_3, the TiO_2(1 0 1) surface is enriched with OH groups. This is in agreement with the *in situ* DRIFTS experiments [1], since strong OH/water vibrations are always visible after reaction.

4.2. Comparison of the proposed reaction pathways for HNCO hydrolysis

Fig. 11 shows a comparison of the new reaction pathway with our previously described mechanism [19] for the isocyanic acid hydrolysis at the ideal (1 0 1) surface of the anatase phase of TiO_2. On the basis of the DFT calculations two reaction pathways are possible. One mechanism proceeds via the molecular adsorption of isocyanic acid and the formation of an intermediate surface complex (see Fig. 11, path 1) [19]. It can occur when water is not present at the beginning of the reaction. By the molecular adsorption of HNCO, an energetically stable intermediate surface complex is created, in which the HNCO skeleton is changing due to new strong bonds between $C–O_s$ and $N–Ti_s$. After decomposition of the intermediate complex and CO_2 desorption a surface oxygen vacancy is formed, on which water adsorbs and NH_3 is successively formed. Although this reaction pathway is conceivable based on the energetic level calculations, it is less probable in real combustion engines due to the high water concentrations in the exhaust gas.

The second mechanism with water being involved at an early stage, presented in this paper (see Fig. 11, path 2), seems to be better suited to real conditions with up to 10% water in the gas phase, and hence, much water on the catalyst surface. Moreover, the reaction intermediates appearing in the course

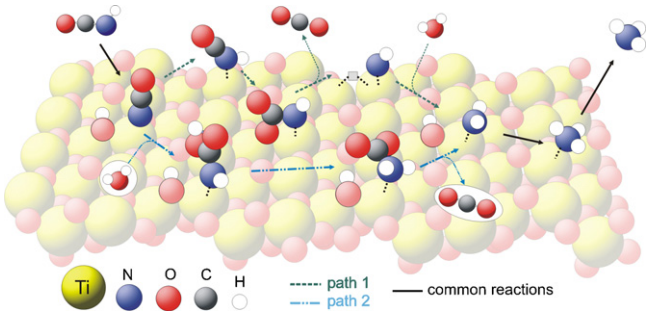

Fig. 11. Schematic comparison of the possible reaction pathways for the isocyanic acid hydrolysis at the (1 0 1) surface of TiO_2: pathway 1 via molecular adsorption of isocyanic acid and pathway 2 via dissociative adsorption of isocyanic acid.

of the reaction (namely carbamic acid, carbamates, amines, etc.) and the reaction steps involved (e.g. hydrogen transfers, decarboxylation and others) are well-known from literature and typical for the chemistry of isocyanic acid and its related compounds. These similarities further increase the plausibility of the proposed mechanism. Reaction path 2 is also more likely due to the lower energy barriers compared to reaction path 1.

The kinetic analysis of the HNCO hydrolysis over TiO_2 revealed a second order reaction, first order with respect to HNCO and first order with respect to water, which is also in agreement with the pathway 2 where both HNCO and water enter the reaction mechanism before the main energy barrier. However, when water was fed in excess according to real conditions, the reaction order was reduced to zero, which proves that the catalyst is covered with water under reaction conditions. The reaction rate was slightly inhibited by the ammonia concentration, especially at very low temperatures. This behavior appears to be plausible, since ammonia desorption at the end of the reaction mechanism requires a significant activation energy. Even when the first barriers in the energy diagram are overcome, ammonia can accumulate in the desorption step, thus inhibiting the overall reaction sequence.

5. Conclusions

DFT calculations show that the hydrolysis of isocyanic acid over the ideal TiO_2(1 0 1) surface occurs with a lower energy barrier than the energy necessary to split the isocyanic acid molecule in the gas phase at the N–C bond, which is the weakest bond in the molecule. In all calculated reaction mechanisms surface O(2)–Ti(5) couples and neighboring Ti(5) centers were involved. It turned out from the calculations that both a dissociative and a molecular adsorption of HNCO is possible, but their role in the hydrolysis of HNCO strongly depends on the availability of water in particular reaction steps.

Under practice-relevant conditions, the reaction pathway with an early influence of water and dissociatively adsorbed HNCO is much more likely than the pathway with molecularly adsorbed HNCO not only due to the generally lower energy barriers of its reaction steps but also due to the good agreement with all experimental results. The course of the reaction can be summarized as follows: water attacks the –NCO group and a carbamic acid complex is formed at the surface in an exothermic reaction without an energy barrier. Then, the carbamic acid is transformed into a carbamate complex, which leads to CO_2 desorption and the formation of an NH_2 group. In the last step of the hydrolysis reaction, NH_3 is formed via hydrogen transfer from an OH group or from molecularly adsorbed water, the latter being energetically favored.

Acknowledgements

The calculations were done partially using the unix farm as well as the linux farm at the Paul Scherrer Institute as well as at the Swiss National Supercomputing Centre. We would like to express our thanks to A. Baiker and A. Wokaun for their helpful suggestions.

References

[1] G. Piazzesi, O. Kröcher, M. Elsener, A. Wokaun, Appl. Catal. B 65 (2006) 55.
[2] M. Kleemann, M. Elsener, M. Koebel, A. Wokaun, Ind. Eng. Chem. Res. 39 (2000) 4120.
[3] D.J. Belson, A.N. Strachan, Chem. Soc. Rev. 11 (1982) 41.
[4] M. Koebel, M. Elsener, T. Marti, Combust. Sci. Technol. 121 (1996) 85.
[5] C. Arrouvel, M. Digne, M. Breysse, H. Toulhoat, P. Raybaud, J. Catal. 222 (2004) 152.
[6] C. Arrouvel, H. Toulhoat, M. Breysse, P. Raybaud, J. Catal. 226 (2004) 260.
[7] A. Beltran, J.R. Sambrano, M. Calatayud, F.R. Sensato, J. Andres, Surf. Sci. 490 (2001) 116.
[8] K. Hadjiivanov, D.G. Klissurski, Chem. Soc. Rev. 25 (1996) 61.
[9] A.A. Tsyganenko, V.N. Filimonov, Spectr. Lett. 5 (1972) 477.
[10] G. Ramis, G. Busca, V. Lorenzelli, P. Forzatti, Appl. Catal. 64 (1990) 243.
[11] G. Ramis, G. Busca, V. Lorenzelli, J. Chem. Soc., Faraday Trans. I 83 (1987) 1591.
[12] A. Fernandez, J. Leyrer, A.R. Gonzales-Elipe, G. Munuera, H. Knozinger, J. Catal. 112 (1988) 489.
[13] G. Busca, H. Saussey, O. Saur, J. Lavalley, V. Lorenzelli, Appl. Catal. 14 (1995) 245.
[14] T. Bredow, K. Jug, Surf. Sci. 327 (1995) 398.
[15] F. Solymosi, J. Rasko, J. Catal. 65 (1980) 235.
[16] F. Solymosi, T. Bansagi, J. Phys. Chem. 83 (1979) 552.
[17] M.M. Branda, P.G. Belelli, R.M. Ferullo, N.J. Castellani, Catal. Today 85 (2003) 153.
[18] H. Gao, H. He, Spectrochim. Acta A 61 (2005) 1233.
[19] I. Czekaj, G. Piazzesi, O. Kröcher, A. Wokaun, Surf. Sci. 600 (2006) 5158.
[20] N.V. Kaminskaia, N.M. Kosti, Inorg. Chem. 37 (1998) 4302.
[21] D. Kaur, P. Sharma, P.V. Bharatam, J. Mol. Struct.: THEOCHEM 757 (2005) 149.
[22] R.K. Khanna, M.H. Moore, Spectrochim. Acta A 55 (1999) 961.
[23] N. Wen, M.H. Brooker, J. Phys. Chem. 99 (1995) 359.
[24] M. Remko, B.M. Rode, J. Mol. Struct.: THEOCHEM 339 (1995) 125.
[25] The program package StoBe is a modified version of the DFT-LCGTO program package DeMon, originally developed by A. St.-Amant and D. Salahub (University of Montreal), with extensions by L.G.M. Pettersson and K. Hermann.
[26] J.P. Perdew, K. Burke, M. Ernzerhof, Phys. Rev. Lett. 77 (1996) 3865.
[27] B. Hammer, L.B. Hansen, J.K. Norskov, Phys. Rev. B 59 (1999) 7413.
[28] J.K. Labanowski, J.W. Anzelm (Eds.), Density Functional Methods in Chemistry, Springer, New York, 1991.
[29] N. Godbout, D.R. Salahub, J. Andzelm, E. Wimmer, Can. J. Phys. 70 (1992) 560.
[30] R.S. Mulliken, J. Chem. Phys. 23 (1955) 1833, 1841, 2388, 2343.
[31] I. Mayer, Chem. Phys. Lett. 97 (1983) 270.
[32] I. Mayer, J. Mol. Struct.: THEOCHEM 149 (1987) 81.
[33] C. Friedrich, Geometrische, elektronische und vibronische Eigenschaften der reinen und defektbehafteten V_2O_5(0 1 0)-Oberfläche und deren Wechselwirkung mit Adsorbaten: Theoretische Untersuchungen, FU, Berlin, 2004.
[34] R. Lemus, Vibrational excitations in H_2O in the framework of a local model, J. Mol. Spectrosc. 225 (2004) 73.
[35] A. Janca, K. Tereszchuk, P.F. Bernath, N.F. Zobov, S.V. Shirin, O.L. Polyansky, J. Tennyson, J. Mol. Spectrosc. 219 (2003) 132.
[36] P. Bour, Chem. Phys. Lett. 365 (2002) 82.

[37] S. Raunier, T. Chiavassa, A. Allouche, F. Marinelli, J.P. Aycard, Chem. Phys. 288 (2003) 197.
[38] I. Onal, S. Soyer, S. Senkan, Surf. Sci. 600 (2006) 2457.
[39] A. Vittadini, A. Selloni, F.P. Rotzinger, M. Gratzel, Phys. Rev. Lett. 81 (1998) 2954.
[40] A. Selloni, A. Vittadini, M. Grätzel, Surf. Sci. 402–404 (1998) 219.
[41] A. Tilocca, A. Selloni, J. Chem. Phys. 119 (2003) 7445.
[42] P.C. Redfern, P. Zapol, L.A. Curtiss, T. Rajh, M.C. Thurnauer, J. Phys. Chem. B 107 (2003) 11419.
[43] D. Eisenberg, W. Kauzmann, The Structure and Properties of Water, Oxford University Press, London, 1969.
[44] J.-L. Leviel, Y. Marechal, J. Chem. Phys. 54 (1971) 1104.
[45] P. Hauck, A. Jentys, J.A. Lercher, Catal. Today 127 (2007) 165.